

---

# MARINE SCIENCES

---

# **Upper Ocean Geostrophic Current and Volume Transport Across Meridional Transects in the Indian Sector of Southern Ocean**

**S.M. Pednekar**

National Centre for Antarctic and Ocean Research, Goa

## **ABSTRACT**

The investigation carried out to understand the upper ocean circulation along two meridional transects (Track-1 and Track-2) using XCTD profiles. Noise factor removed from the each profile manually and further interpolation carried out to get final product. In general, sea surface temperature and sea surface salinity at 1 m depth decreasing southward with salinity fluctuation seen south of 46°S. Along Track-1 thermal structure of temperature and salinity showing sinking and rising of isotherms and isohalines, respectively making wave like pattern between 35°S -39°S, where ocean current are opposite. South of 39°S, isotherms are more inclined and water is mixing with different physical properties. Cold ( 0°C) water penetrates northward in subsurface region (100 m) north of 55°S. Along Track-2 north of 39°S wave pattern repeated and south of it isolines are running vertical until 42.5°S. Isotherms and isohalines are parallel to each other in top 250 m from 43°S to 55°S. Intrusion of cold ( 0°C) water tough identified at 150-350 m south of 53°S. From the wave like pattern observed along Track-1 and Track-2 in 500 m from 35°S to 39°S, it is understood that the Agulhas Current (AC) in December, 2007 crossing the Track-1 in between 35°S to 39°S and turns back as Agulhas Return Current (ARC) current due formation of anti-cyclonic warm core mesoscale eddy having positive vorticity. Since Track-2 was occupied in March, 2008 the southern core of the ARC shift more south (40°S). Intrusion of cold ( 0°C) water found in top 100 m along Track-1 is deepens to 250-350 m along Track-2. The geostrophic integrated net volume transport in the upper 500 m varying between 0.3 to 4.5 Sv and 0.2 to 7.5 Sv along Track-1 and Track-2, respectively where the flow of the current is eastwards (+ve) and westward (-ve). North of 40°S net transports are found more as compare to south of it. Further improvement in technique of data acquisition as well processing methodology is required to improved errors in data collection and profiles editing so that we understand processes of the southern ocean.

**Keywords:** Hydrographic Parameters, Geostrophic Current, Volume Transport.

## **1.0 INTRODUCTION**

The Indian sectors of Southern Ocean (SO) region play a major role in Global Circulation belt. The formation and mixing of the water masses

in the polar region cause changes in the northward flow of the meridional overturning circulation and as a consequence, in the Earth Climate system. SO is a unique in its characteristic and circumpolar region embedded with fronts within the Antarctic Circumpolar Current (ACC), having the key role in modulating the present hydrographic condition. The ACC is largely influenced by the surrounding oceanographic regimes to its northern and southern boundaries. The horizontal spatial gradients in current speed (Sparrow et al., 1996), temperature, salinity and density (Belkin and Gordon, 1996; Park et al., 2001; Orsi et al., 1995), as well as enhanced vertical circulation associated with bathymetric features (Orsi et al., 1995; Anilkumar et al., 2007). Major fronts of the ACC comprise of Sub Antarctic Front (SAF) and Polar Front (PF), which form the northern and southern boundaries of the Polar Frontal Zone, respectively (Whitworth and Nowlin, 1987). Model studies and historical data suggest that the SO sector between Africa and Antarctica has particular variety in the position and strength of frontal currents (Sparrow et al., 1996; Belkin and Gordon, 1996). The study of SO is important because of a number of reasons related to atmospheric and oceanographic features. Wind-driven anticyclonic gyre of the South Indian Ocean (SIO) where most of the water re-circulates in the western and central parts of the SIO basin (Stramma and Lutjeharms, 1997), which is a distinct feature of the SIO.

Most of the investigations carried out in the SO are concentrated on the central and eastern Indian Ocean sector (Rintoul et al., 1997; Rintoul et al., 2002; Rintoul and Bullister, 1999; Rintoul and Sokolov, 2001; Sokolov and Rintoul, 2002; Yuan et al., 2004). The SO is lacking in hydrodynamics study and to overcome this problem we have operated expendable-conductivity-temperature-depth (XCTD) during the austral summer (December, 2007 to March, 2008) namely, Cape Town to India Bay, Antarctica i.e. southwest Indian Ocean Sector (Track-1) and from Prydz Bay, Antarctica to Cape Town i.e. southeast Indian Ocean Sector (Track-2) during Indian Scientific Expedition to Antarctica (ISEA-27). The investigation carried out to understand the upper ocean hydrodynamics along two meridional transects (Track-1 and Track-2). The aim of this study is to understand upper ocean circulation and volume transport across ship routes. From the **Fig. 1** it is understood that the bottom topography of the SO showing variation in depth, basins etc and highlighting the topographic features. The in-situ data sets and the methods are described in Section 2, while Section 3 gives the results and discussions. Finally, summary are drawn in Section 4.

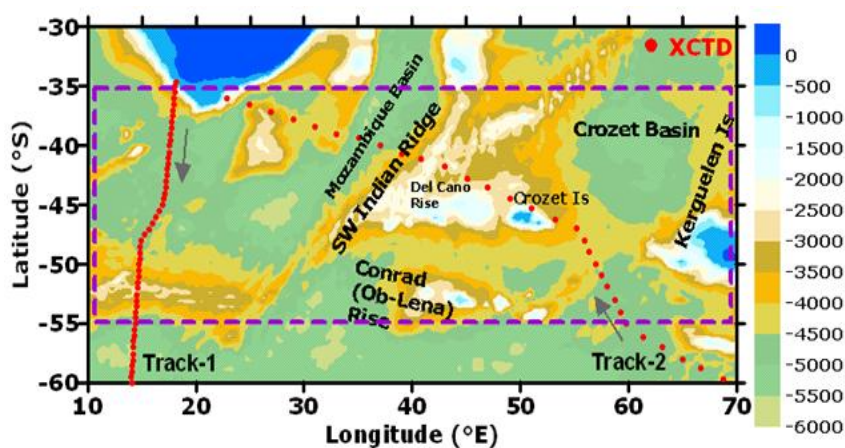


Fig. 1: Map showing ship Track-1 from Cape Town to India Bay, Antarctica and Track-2 from Prydz Bay, Antarctica to Cape Town overlapped with bottom topography. The XCTD stations operated along two tracks symbol during austral summer of 2007-08 are shown in solid dot. The contours intervals shown are 500 m and dashed square box indicates the study region where topography changes are seen

## 2.0 DATA AND METHODS

Under 27th Indian Scientific Expedition to Antarctica we operated XCTD (expendable conductivity - temperature - depth) probes along the ship's route from Cape Town to New India Bay and from Prydz Bay to Cape Town in one degree interval without stopping the vessel. The vertical profiles of temperature and conductivity were recorded using PC based MK-21 Sippican system up to 1000 m water column. The XCTD (make: Tsurumi Seiki Company Limited, Japan; type: XCTD; terminal depth: 1000 m; temperature/ salinity accuracy:  $\pm 0.02$  °C/ $\pm 0.03$  mS cm<sup>-1</sup>) to record vertical profiles of temperature and salinity along the ship track (Fig. 1). When the probes are falling through the water column spikes may occur at some depths in the vertical profiles of the temperature and salinity data. Such spikes in the density vertical profiles are removed in present study while processing. The survey track from Cape Town to Antarctica was surveyed during last week of December, 2007 (Track-1) and the return journey from Prydz Bay to Cape Town was occupied during mid-March, 2008 (Track-2). A comparison of XCTD and Sea Bird CTD profiles revealed that the former is consistent with temperature and salinity accuracy specified by the manufacturer (Mizuno and Watanabe, 1998), and the fall rate for the XCTD probes showed no systematic bias in the fall equation provided by the manufacturer (Kizu et al., 2008). The

temperature profiles were quality controlled by following the standard procedures (Bailey et al., 1993). High frequency noise in the salinity profiles was minimized by using a median filter with a 20 m window (Xiaojun et al., 2004). The geostrophic velocity across a pair of hydrographic stations was computed by using the method of Pond and Pickard, (1983) relative to the 500 db level of no motion (equation 1).

$$v = \frac{1}{f} \int_{500}^0 \Delta\Phi dz \quad \dots(1)$$

where  $f = 2 \Omega \sin \theta$  is the Coriolis parameter( $s^{-1}$ ) at a mean latitude  $\theta$ ,  $\Omega = 7.272 \times 10^{-5} \text{ rad.s}^{-1}$  is the rotation rate of the earth,  $dz$  is the depth interval (m) and  $\Delta\phi$  is the geopotential anomaly ( $m^2s^{-2}$ ) between adjacent pair of XCTD stations.

### 3.0 DISCUSSION

Indian Scientific Expedition to Antarctica launched during December 2007 to March 2008, austral summer. The cruise started from Cape Town last week of December 2007. Fig. 2 showing the distribution of surface oceanographic parameters in the Indian Ocean sector of SO along the ship Track-1 from Cape Town to New India Bay (Fig. 2a) in  $1^\circ$  latitudinal belt from  $35^\circ\text{S}$  to  $55^\circ\text{S}$ . The distribution of SST (Fig. 2a) and Sea Surface Salinity (SSS) (Fig. 2b) at 1 m depth from the XCTD profiles showing varying pattern. The SST remains constant up to  $39^\circ\text{S}$  and decreasing towards south from  $21^\circ\text{C}$  to  $0^\circ\text{C}$ . The distribution of SSS varies along ship track from 28.9 psu to 33.3 psu.

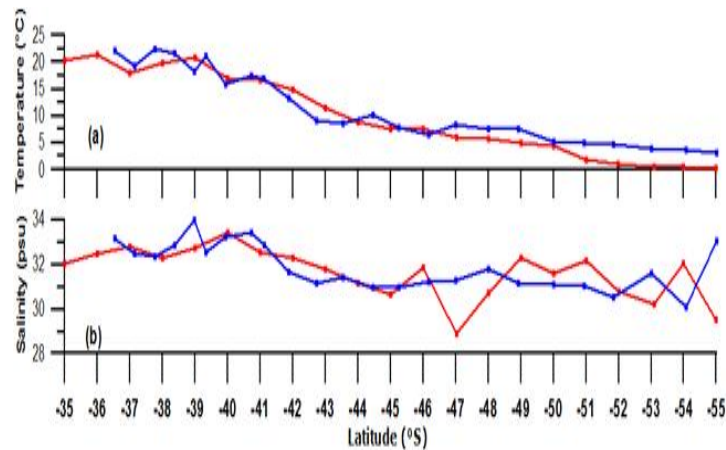


Fig. 2: Distribution of surface (a) temperature ( $^\circ\text{C}$ ) and (b) salinity at 1m depth along Track-1 (red color) and Track-2 (blue color) from XCTD profiles

### 3.1 Hydrographic Characteristics Along Track-1

The distribution of vertical structure of temperature, salinity and geostrophic current along Track-1 are shown in Fig. 3a, 3b, and 3c, respectively from Cape Town to New India Bay in top 500 m water column. In Fig. 3a based on incline nature of isotherms in the water column it was predicted that the warmer water moves southwards and colder water extend northward in the deeper depth. The isotherms in Fig. 3a showing wave like pattern between 35°-40°S and sinking at 36°S and 39°S from surface to 500 m depth. Holliday and Reed, (1998) also found such wave pattern between 38°-39°S in their study. The wavy like pattern of temperature and salinity isolines observed from 31° to 37°S (Anilkumar et al., 2007) is due to the effect of southwest Indian ridge. Section 48°E shows a particularly good example of a cold-core (cyclonic) eddy at 37°-39°S centre at 38°S showing sinking of temperature isolines which was earlier shown between 37-38°S, 46°E in a satellite-derived sea surface temperature image of that area during the cruise (Fig. 10b of Pollard et al., 1995), where the front crosses the topographic high of the SW Indian Ridge. South of 39°S gradient in isotherm is more observed in the upper 500 m water column. The region of strong gradient in temperature vertically is identified as the ACC region where forms different types of water masses. Identification of the main ACC fronts is essential in order to trace the upper-level circulation associated with strong baroclinic shear (Nowlin and Klinck, 1986), and to mark the boundaries of different water masses. North of 55°S in top 100 m a tough of cold water below 0°C intrudes northward and its approaching influence is noticed until 50°S.

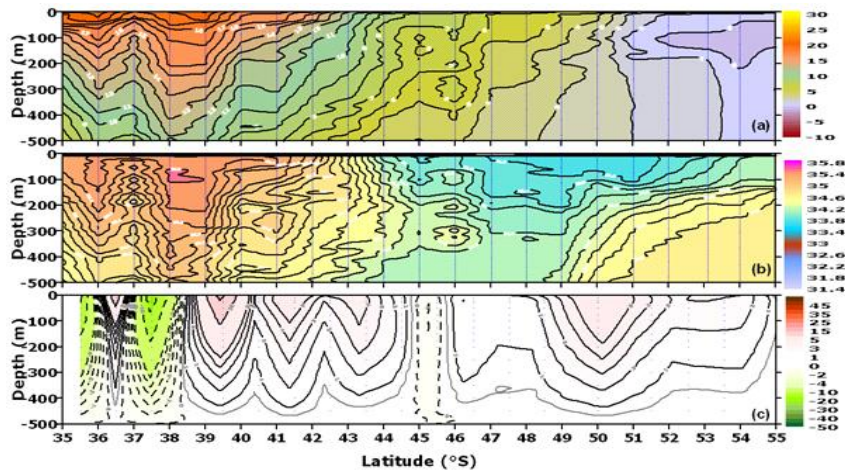


Fig. 3: Vertical structure of (a) Temperature ( $^{\circ}\text{C}$ ), (b) Salinity, and (c) Geostrophic current ( $\text{cm s}^{-1}$ ) along meridional hydrographic Track-1

Fig. 3b showing the vertical structure of salinity along Track-1, which represents similar pattern of isohaline (Fig. 3a) except in top 100 m north of 55°S. In this paper here and below no unit is assigned to salinity because it is measured from the ratio of conductivities. North of 39°S wave pattern showing sinking of isohaline 35.4 and 35.5 at 36° and 38.5°S, respectively. South of 40°S strong gradient of isohaline observed until 45°S with mixing pockets of higher salinity below 150 m depth. Low salinity waters ( $\leq 33.8$ ) sinking from surface to a deeper depth between 45° to 49°S and penetrates northward. Luis and Pednekar, (2010) noticed that the Track 1 passes over prominent anticyclone centered at 38.7°S, which is marked by surface topography of 2.7 dyn m, surface temperature of 20°C and salinity of 35.5 and an oval-shaped eddy which is shed from the AR has diameter of  $\sim 200$  km in the north-south direction. The higher gradients in surface temperature and sigma-t centered on 37°S reflects the presence of a cyclone which is characterized by an enhanced surface elevation of  $\sim 2.1$  dyn m; it exchanges warm (21°C) and saline 35.4. The distribution of geostrophic velocity in the top 500 m water column is shown in Fig. 3c. The dashed contours representing westward flow and solid contours represents eastward flow of current system in the upper 500 m water column. Between 35.5°–39°S the direction of the current is westward and eastward with maximum speed of  $\geq 16$  cm s<sup>-1</sup> and 14 cm s<sup>-1</sup>, respectively. Between 38.5° to 45°S the direction of the current showing eastward with maximum core located at 39.5°S 41.5°S and 43.5°S with a speed of  $\geq 10$  cm s<sup>-1</sup>,  $\geq 05$  cm s<sup>-1</sup>, and  $\geq 04$  cm s<sup>-1</sup>, respectively. Between 45° to 48°S weak westward flow and in continuation weak eastward flow  $\geq 5$  cm s<sup>-1</sup> at 50°S) noticed south of 48°S.

### 3.2 Hydrographic Characteristics Along Track-2

Figs. 4a, 4b, and 4c represent hydrographic vertical characteristics of temperature, salinity and geostrophic velocity along Track-2. As compared to Track-1, Track-2 passing through large variations in bottom topography and shallow region (Fig. 1) where as Track-1 passing through open ocean with less variation in bottom topography. Hence it should be noted that there is topographic conditions do have influence on physical parameters (Anilkumar et al., 2007). The vertical temperature structure (Fig. 4a) in the upper 500 m water column north of 55°S showing wave pattern and sinking of isotherms north of 39°S. Strong vertical gradient observed between 41° to 43°S and south of it in top 200 m isotherms with temperature  $\geq 4^\circ\text{C}$  are running parallel to surface until 55°S. Penetrations of water with temperature  $\leq 2^\circ\text{C}$  is seen at 250 to 350 m depth water column. Pockets of warm (23°C) and saline (35.4) water of Southern

Subtropical Surface Water (STSW) (Valentine et al., 1993) are detected in the AC core identified at 36°S (Fig. 4a). The AC has a width of about 100 km. The pockets of high salinity (35.5) and warm (~19 °C) in the upper 300 m and downwelling signature centered at 37.5°S corresponds to an anticyclonic eddy in the ARC characterized by elevated surface topography (2.7 dy m) as revealed by Luis and Pednekar, (2010). The ARC and the Subtropical Convergence sometimes overlap, as a result of which the meridional property gradients are markedly increased and instabilities due to strong current shear produce a range of mesoscale eddies (Lutjeharms and Valentine, 1988). Southern Sub Tropical Front is also characterized by surface divergence indicative of upwelling, the Crozet Basin area is known for a peculiar circulation pattern compared to the other sectors of the SO, because of the confluence of ARF, Sub Tropical Front and Sub Antarctic Front that occurs in the band 40°-43°S (Park et al., 1993). The vertical salinity structures for Track-2 are portrayed in Fig. 4b and the structure representing vertical temperature structure (Fig. 4a). As similar to Fig. 3b, isohaline of  $\leq 35.4$  and  $\leq 35.5$  showing sinking at 36.5°S and 38°S, respectively which is continuing until 500 m (Fig. 4b). Isohaline contours of salinity 34.1 to 34.8 are running parallel to each other vertically between 41° to 43°S. South of 43°S isohalines are running parallel to each other from surface to 500 m until 55°S. The melt water marked by low salinity (~34) in the upper 30 m pushes the high salinity water below 50 m.

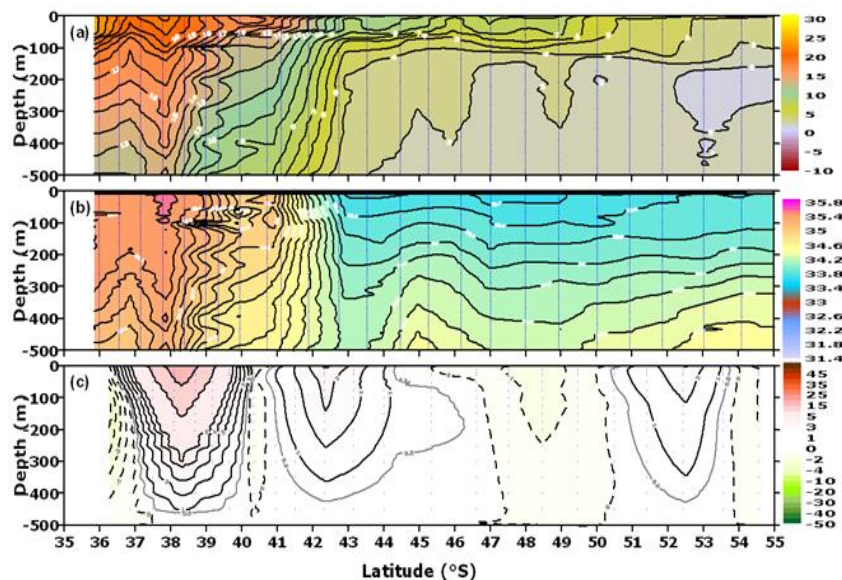


Fig. 4: Same as Figure 3, but for the Track-2

The wintertime observations of Middleton and Humphries (1989) indicate that the Prydz Bay shelf is occupied by saltiest water of salinity slightly higher than 34.6. The distribution of relative velocity with reference to 500 m water column computation is shown in Fig. 4c. The vertical structure of geostrophic current showing direction as well speeds of the current in zonal direction. There exists eastward flow of current at 36.5°S with a speed of  $> 1 \text{ cm s}^{-1}$ . Between 36° to 40.8°S the direction of current changes to westward with a speed of  $\geq 25 \text{ cm s}^{-1}$  at 38.8°S. In top  $\sim 300 \text{ m}$  water column a weak eastward shallow current with  $\sim 0.5 \text{ cm s}^{-1}$  identified at 41°S, at 49°S and at 54.5°S. A core of the westward current located at 43°S and 52.5°S with speed of  $\geq 2 \text{ cm s}^{-1}$ .

### 3.3 Net Barotropic Volume Transports

Fig. 5 showing the meridional distribution of net barotropic volume transports (bar chart) integrated referenced to the common level of 500 db across Track-1 (Fig. 5a) during December, 2007 and Track-2 during March, 2008 (Fig. 5b). A negative transport is directed towards west or southwest and positive transport directed towards east or southeast. The direction of the net volume transport changes according to the direction of relative current along two transects having different topographic features. Westward transport of 4 Sv and eastward transport of 2 Sv present between 35°S to 38°S in Fig. 5a. Wave like nature of isotherms (Fig. 3a) and isohalines (Fig. 3b) were identified from surface to 500 m. Eastward transport noticed between 39°S to 45°S with maximum at 39.5°S (3.6 Sv), 41.5°S (2.1 Sv) and 43.5°S (1.7 Sv) rest are weak transports. A weak transports identified at 45.5°S (0.6 Sv) and eastward transport south of it with maximum at 50°S (4.5 Sv). Solid line showing integrated surface geostrophic speed varies between  $0.1 \text{ cm s}^{-1}$  to  $20 \text{ cm s}^{-1}$  which is following the direction of the transport. It is pertinent to note that the mean barotropic volume transport relative to 2500 db estimated in the literature across sections near the Greenwich Meridian using different methods ranges from 87.5 to 109.6 Sv (Rintoul et al., 2002; Legeais et al., 2005). Of 36 Sv, about 90% (32 Sv) is associated with the ACC in the belt 43°–57.2°S. Luis and Pednekar (2010) investigated the westward transport associated with anticyclones at 35.5°, 37° and 38.7° amounts to 3.2, 11.3 and 2.8 Sv, respectively. This amount (17 Sv) is comparable to the Agulhas leakage of 15 Sv that has been estimated from drifters and floats in the upper 1000 m (Richardson, 2007). The reported range of AC transport in the literature varies from 25 to 35 Sv (Harris, 1972; Stramma and Lutjeharms, 1997). The transport estimated in the present study is small compared to literature

could be due to shallow reference level of no motion considered while computing geostrophic calculation.

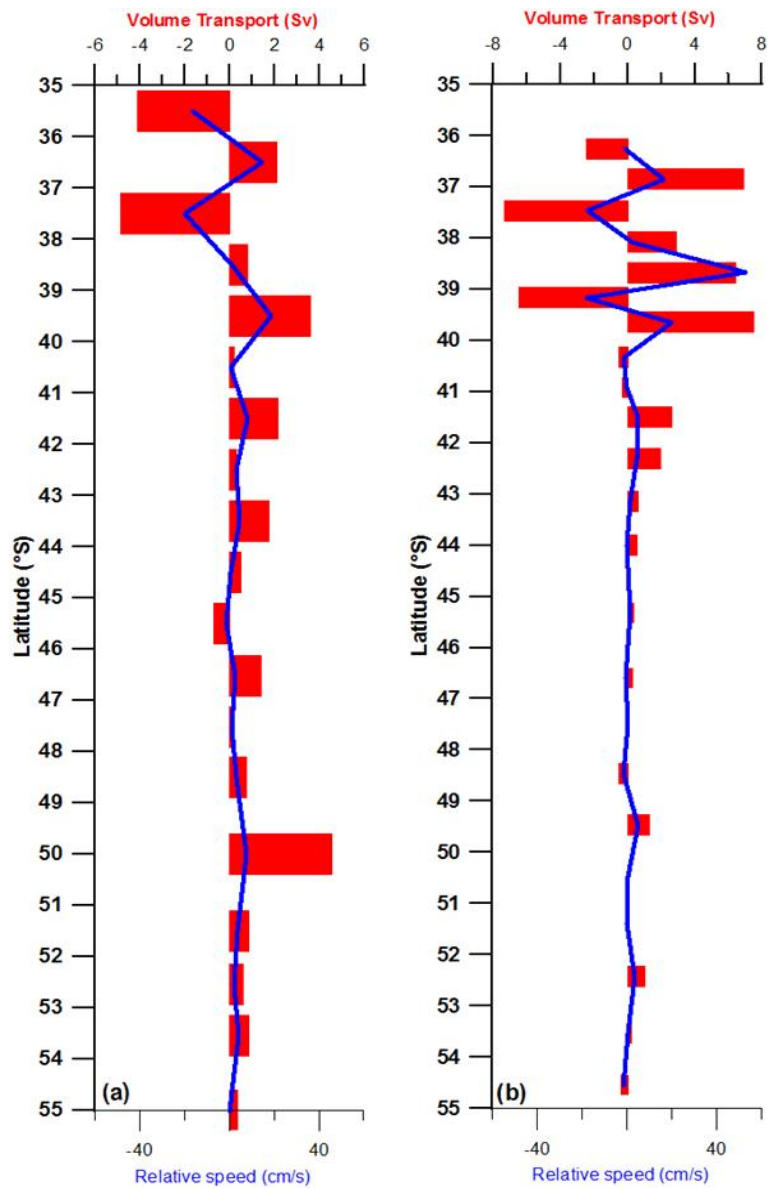


Fig. 5: Surface geostrophic speeds (solid blue line) in  $\text{cm s}^{-1}$ , Net volume transports (red bar chart) in Sv ( $1\text{Sv} = 10^6 \text{ m}^3 \text{ s}^{-1}$ ) (a) Track-1 during December, 2007 and (b) Track-2 during to March, 2008

In Fig. 5b the estimated integrated volume transport in the upper 500 m is varying between 0.5 Sv to ~7 Sv shows eastward and westward flow pattern similar to Fig. 5a. As compared to Track-1 (Fig. 5a) the transport estimated between 35°S and 40°S are more and the direction changes eastward and westward. Westward transport of 2.5 Sv and 7.3 Sv at 36.2°S and 37.5°S and eastward transport of 6.9 Sv identified at 36.8°S, respectively. Similarly eastward transport of 2.8 Sv, 6.4 Sv and 7.5 Sv are estimated at 38°S, 38.8°S and 39.7°S, respectively. There exists westward transport of 6.4 Sv at 39.2°S. The relative surface speed of along Track-2 is represented in solid line which follows direction of transport (Fig. 5b). Luis and Pednekar (2010) noted that occurrence of an opposing transport in close proximity in the region spanning 44°-48°S (east Crozet Basin) is attributed to the meridional meandering dictated by potential vorticity and abetted by the mesoscale eddy activity induced by strong winds ( $\sim 17 \text{ ms}^{-1}$ ). However, the transport observed south of 59° can be attributed to the mesoscale eddy activity along both tracks, which was previously reported along 30°E section, between 51° and 59°S (Park et al., 2001). Earlier investigator reported 23 Sv between 40°-43°S on 45°E section (Anilkumar et al, 2007), where as it was reported  $< 20$  Sv by Park et al, (1993) and Orsi et al, (1995) but in this range we investigated variability of transport associated with the fronts on 48°E. There is variation in flow direction and transport could be due to the geostrophic flow exhibited a cyclonic or anticyclonic circulation possibly due to the influence of the topographic features (Fig. 1).

#### 4.0 CONCLUSIONS

In-situ XCTD (expendable conductivity-temperature-depth) observations were carried out along the two meridional transects namely Cape Town to India Bay, Antarctica i.e. southwest Indian Ocean Sector and from Prydz Bay, Antarctica to Cape Town i.e. southeast Indian Ocean Sector during Indian Scientific Expedition to Antarctica (ISEA-27) during austral summer of 2007-08. Hydrographic XCTD density profiles operated were used in this study of the SO to improve our knowledge of the dynamics in the ACC region. The objective of the paper is to use the data collected along two meridional transects to investigate the circulation current system and geostrophic volume transport. The distribution of SST and SSS at 1 m depth from the XCTD profiles showing varying pattern. The SST remains constant up to 39°S and decreasing towards south from 21°C to 0°C. The distribution of SSS varies along ship track from 28.9 psu to 33.3 psu. From the Track-1 it was understood that warmer water moves southwards on top and colder water extend northward in the deeper depth.

Wave like nature of isotherms and isohalines pattern detected between 35°-40°S and sinking of isolines at 36°S and 39°S from surface to 500 m depth along both survey Tracks. In Track-1 north of 55°S a tongue of cold water below 0°C intrudes northward and its approaching 51°S in top 100 m whereas in Track-1 it was deepens to 250-300 m. As compared to Track 1 strong vertical gradient observed between 41° to 43°S and south of it isotherms with temperature  $\geq 4^\circ\text{C}$  are running parallel to surface until 55°S in top 200 m. The southward shift in the frontal positions is attributed to the influence of the ridges that dominate the seafloor topography in that region. The rotational tendency of waters in the study area (attributed to the seabed topography) is perhaps driven by the eastward flowing Antarctic Circumpolar Current resulting in a southward shifting of frontal structures. Geostrophic zonal speed and integrated volume transport computed relative to 500 db level along the two transects reveals that the large volume transports and strong speed associated within the current. Eastward and westward flow noticed on both the meridional sections.

### Acknowledgements

I am grateful to the Ministry of Earth Sciences for the financial grant for XCTD probes and to the Director, NCAOR for his encouragement to pursue these studies. I acknowledge Project Investigators Dr. M. Sudhakar as well Dr. N. Anilkumar for their support extended during cruise period.

### REFERENCES

1. Anilkumar, N., Pednekar, S.M., Sudhakar, M., 2007. Influence of ridges on hydrological parameters in the southwest Indian Ocean. *Mar. Geophys. Res.* 28, 191-199.
2. Aoki S, Kazunori Akitomo. 2007. Observations of small scale disturbances of the Subantarctic Front south of Australia, *Deep-Sea Research Part I*, v 54: 320-339.
3. Bailey, R., Gronell, A., Phillips, H., Meyers, G., Tanner, E., 1993. CSIRO Cookbook for Quality Control of Expendable Bathythermograph (XBT) Data, CSIRO Marine Laboratories Report 221, CSIRO, Hobart.
4. Belkin, I.M., Gordon, A.L., 1996. Southern Ocean fronts from the Greenwich Meridian to Tasmania. *J. Geophys. Res.* 101, 3675-3696.
5. Gao Guoping, Han Shuzong, Dong Zhaoqian, et al., 2003. Structure and variability of fronts in the South Indian Ocean along sections from Zhongshan Station to Fremantle. *Acta Oceanologica Sinica*, 25(6): 9-19.
6. Harris, T.F.W., 1972. Sources of the Agulhas Current in spring of 1964. *Deep-Sea Res.* 19 (9), 633-650.
7. Holliday, N.P., Reed, J.F., 1998. Surface oceanic fronts between Africa and Antarctica. *Deep-Sea Res. Part 1* 45, 217-238.

8. Kizu, S., Onishi, H., Suga, T., Hanawa, K., Watanabe, T., Iwamiya, H., 2008. Evaluation of the fall rates of the present and developmental XCTDs. *Deep-Sea Res. Part 1* 55, 571-586.
9. Legeais, J.F., Speich, S., Arhan, M., Ansorge, I.J., Fahrbach, E., Garzoli, S., Klepikov, A., 2005. The baroclinic transport of the Antarctic Circumpolar Current south of Africa. *Geophys. Res. Lett.* 32, L2460210.1029/2005GL023271.
10. Luis A.J. and S.M. Pednekar, 2010. Hydrodynamics between Africa and Antarctica during Austral summer 2008. *Journal of Marine Systems*, 1-13.
11. Lutjeharms, J.R.E., Roberts, H.R., 1988. The Natal Pulse: an extreme transient of the Agulhas Current. *J. Geophys. Res.* 93, 631-645.
12. Middleton, J.H., Humphries, S.E., 1989. Thermocline structure and mixing in the region of Prydz Bay, Antarctica. *Deep-Sea Res. Part 1. Oceanogr. Res. Pap.* 36, 1255-1266.
13. Mizuno, K., Watanabe, T., 1998. Preliminary results of in situ XCTD/CTD comparison test. *J. Oceanogr.* 54, 373-380.
14. Nowlin, W.D., Klinck, J.M., 1986. The physics of the Antarctic Circumpolar Current. *Rev. Geophys.* 24, 469-491.
15. Orsi, A.H., Nowlin Jr., W.D., Whitworth, T., 1993. On the circulation and stratification of the Weddell Gyre. *Deep-Sea Res. Part 1* 40, 169-203.
16. Orsi, A.H., Whitworth III, T., Nowlin Jr., W.D., 1995. On the meridional extent and fronts of the Antarctic Circumpolar Current. *Deep-Sea Res. Part 1. Oceanogr. Res. Pap.* 45, 641-673.
17. Park, Y.H., Gamberoni, L., Charriaud, E., 1993. Frontal structure, water masses, and circulation in the Crozet Basin. *J. Geophys. Res.* 98, 12361-12385.
18. Park, Y.H., Charriaud, E., Craneguy, P., 2001. Fronts, transport, and Weddell Gyre at 30°E between Africa and Antarctica. *J. Geophys. Res.* 106, 2857-2879.
19. Pond, S., Pickard, G.L., 1983. *Introductory Dynamical Oceanography*, Second Ed. Pergamon Press, Oxford.
20. Pollard, R. T., and J. F., Read, 2001. Circulation pathways and transports of the Southern ocean in the vicinity of the southwest Indian Ridge. *Journal of Geophysical Research* 106, C2, 2881-2898.
21. Rintoul, S.R., Donguy, J.R., Roemmich, D.H., 1997. Seasonal evolution of upper thermal structure between Tasmania and Antarctica. *Deep-Sea Research I* 44 (7), 1185-1202.
22. Rintoul, S.R., Bullister, J.L., 1999. A late winter hydrographic section from Tasmania to Antarctica. *Deep-Sea Research I* 46 (8), 1417-1454.
23. Rintoul, S.R., Sokolov, S., 2001. Baroclinic transport variability of the Antarctic Circumpolar Current south of Australia (WOCE repeat section SR3). *Journal of Geophysical Research* 106 (C2), 2815- 2832.
24. Rintoul, S.R., Sokolov, S., Church, J., 2002. A 6-year record of baroclinic transport variability of the Antarctic Circumpolar Current at 140 degrees E derived from expendable bathythermograph and altimeter measurements. *Journal of Geophysical Research-Oceans* 107 (C10) (Art. No. 3155 SEP-OCT).

25. Sokolov, S., Rintoul, S.R., 2002. Structure of southern ocean fronts at 140°E. *Journal of Marine Systems* 37 (1-3), 151-184.
  26. Richardson, P.L., 2007. Agulhas leakage into the Atlantic estimated with subsurface floats and surface drifters. *Deep Sea Res. Part I, Oceanogr. Res. Pap.* 54 (8), 1361-1389.
  27. Rintoul, S.R., Sokolov, S., Church, J., 2002. A 6 year record of baroclinic transport variability of the Antarctic Circumpolar Current at 140°E from expendable bathythermograph and altimetry measurements. *J. Geophys. Res.* 107 (C10), 315510.1029/2001JC000787.
  28. Sparrow, M.D., Heywood, K.J., Brown, J., Stevens, D.P., 1996. Current structure of the south Indian Ocean. *J. Geophys. Res.* 101 (C3), 6377-6391.
  29. Speich, S., Blanke, B., Cai, W., 2007. Atlantic meridional overturning circulation and the Southern Hemisphere supergyre. *Geophys. Res. Lett.* 34, L23614.1029/2007GL031583.
  30. Stramma, L., Lutjeharms, J.R.E., 1997. The flow field of the subtropical gyre of the South Indian Ocean. *J. Geophys. Res.* 102, 5513-5530.
  31. Valentine, H.R., Lutjeharms, J.R.E., Brundrit, G.B., 1993. The water masses and volumetry of the southern Agulhas Current region. *Deep-Sea Res. Part I* 40, 1285-1305.
  32. Whitworth III, T., Nowlin, W.D., 1987. Water masses and currents of the Southern Ocean at the Greenwich Meridian. *J. Geophys. Res.* 92, 6462-6476.
  33. Xiaojun, Y., Douglas, G.M., Zhaoqian, D., 2004. Upper ocean thermohaline structure and its temporal variability in the southeast Indian Ocean. *Deep-Sea Res. Part I* 51, 333-347.
  34. Yuan, X., Martinson, D.G., Dong, Z., 2004. Upper-ocean thermal structure and its temporal variability in the southeast Indian Ocean. *Deep-Sea Research I* 51, 333-347.
-